scientific reports

Check for updates

OPEN

Genetic atlas of hygro-and thermosensory cells in the vinegar fly *Drosophila melanogaster*

Kristina Corthals[1], Vilma Andersson[1], Allison Churcher[2], Johan Reimegård[3] & Anders Enjin[1]✉

The ability of animals to perceive and respond to sensory information is essential for their survival in diverse environments. While much progress has been made in understanding various sensory modalities, the sense of hygrosensation, which involves the detection and response to humidity, remains poorly understood. In this study, we focused on the hygrosensory, and closely related thermosensory, systems in the vinegar fly *Drosophila melanogaster* to unravel the molecular profile of the cells of these senses. Using a transcriptomic analysis of over 37,000 nuclei, we identified twelve distinct clusters of cells corresponding to temperature-sensing arista neurons, humidity-sensing sacculus neurons, and support cells relating to these neurons. By examining the expression of known and novel marker genes, we validated the identity of these clusters and characterized their gene expression profiles. We found that each cell type could be characterized by a unique expression profile of ion channels, GPCR signaling molecules, synaptic vesicle cycle proteins, and cell adhesion molecules. Our findings provide valuable insights into the molecular basis of hygro- and thermosensation. Understanding the mechanisms underlying hygro- and thermosensation may shed light on the broader understanding of sensory systems and their adaptation to different environmental conditions in animals.

The astonishing diversity of sensory systems among animals enables them to navigate and survive in an array of challenging environments. In recent decades, significant progress has been made in unraveling the underlying mechanisms of many of these sensory modalities, however, a few senses remain unknown. One of them is hygrosensation—the ability to detect and respond to humidity. Humidity is a climactic factor crucial for the survival of terrestrial animals[1,2]. Insects in particular are sensitive to variations in humidity and use this ability to guide them in specific behaviors such as food-seeking and oviposition site-selection[3,4].

Humidity is detected by humidity receptor neurons (HRNs), which are located within a specialized sensory structure called the hygrosensillum[5]. In insects, hygrosensilla are found on the antenna, a pair of appendages on the head that functions as a multi-sensory organ detecting temperature, odorants and sound in addition to humidity. The hygrosensilla are intermingled with olfactory sensilla and share their general structure. However, unlike olfactory sensilla, which have pores to enable odorant molecules to reach the sensory receptors, hygrosensilla are covered by a poreless hydrophobic cuticle. As a result, the HRNs are protected from exposure to airborne molecules thereby conferring an enigmatic attribute to the mechanism by which humidity is sensed. Typically, hygrosensilla consist of three types of HRNs: a moist neuron (depolarized by increased humidity), a dry neuron (depolarized by decreased humidity), and a hygrocool neuron (depolarized by decreased temperature), which are co-located within a sensillum, forming a hygrosensory "triad."

In the vinegar fly *Drosophila melanogaster*, the hygrosensilla are found within an invagination of the posterior side of the antenna called the sacculus (Fig. 1A)[6–9]. The sacculus is composed of three chambers, with the initial two dedicated to the detection of humidity while the third chamber contain olfactory receptor neurons (ORNs) that respond to acids and ammonium[10,11]. HRNs express members of the ionotropic receptor (IR) family, dry neurons express Ir40a, while moist neurons express Ir68a. Hygrocool cells found within the first chamber of the sacculus express IR21a, while the hygrocool cells in the second chamber express Ir40a[6–9,12]. Additionally, Ir21a is also expressed within the cold-sensing temperature receptor neurons (TRNs) found in the arista[13]. The arista also contain another type of TRN, the hot cells, that express the gustatory receptor GR28b.d[14]. HRNs and TRNs also express two additional IRs, Ir93a and Ir25a, which may act as co-receptors.

[1]Department of Experimental Medical Science, Lund University, Lund, Sweden. [2]Department of Molecular Biology, National Bioinformatics Infrastructure Sweden, Science for Life Laboratory, Umeå University, 901 87 Umeå, Sweden. [3]Department of Cell and Molecular Biology, National Bioinformatics Infrastructure Sweden, Science for Life Laboratory, Uppsala University, Husargatan 3, 752 37 Uppsala, Sweden. ✉email: anders.enjin@med.lu.se

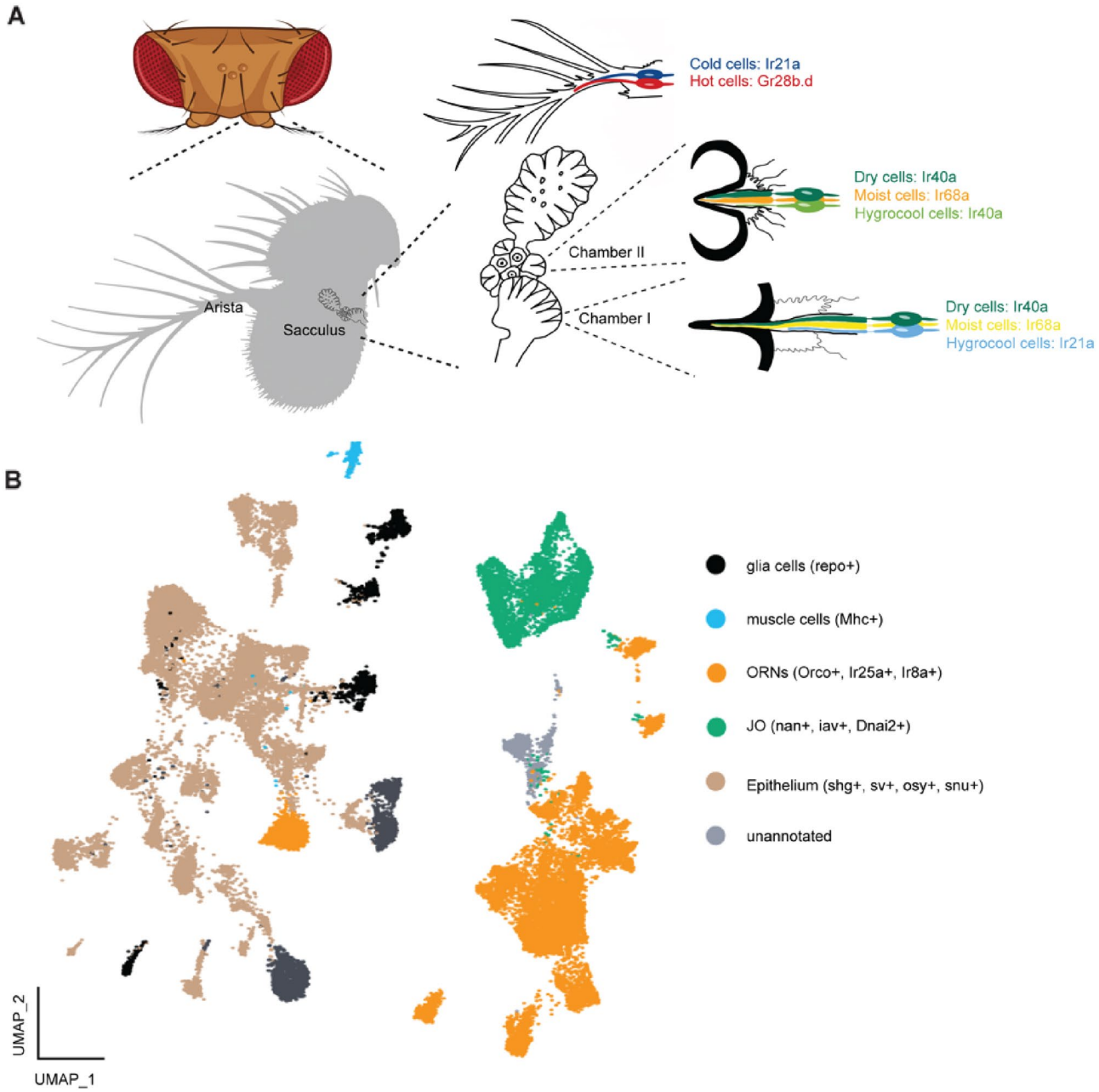

Figure 1. (**A**) Schematic illustration of the temperature and hygrosensory organs in the antenna. Created with biorender.com with inspiration from[15,16]. (**B**) UMAP plot of the whole antennal data set (all segments + arista) with annotations for the different functional groups. ORN: olfactory receptor neurons. JO: Johnstons Organ. One cluster could not be assigned a definite identity, based on gene expression it is suspected to contain ORN and JO neurons.

Although all HRNs and TRNs express a sensory receptor protein, not all cells can be defined by the expression of a unique receptors suggesting other molecules are involved in the transduction mechanism. Here we describe an analysis of the antennal dataset from the fly cell atlas[17], consisting of > 37,000 nuclei. This analysis identified 1411 nuclei which we could classify as arista neurons, sacculus neurons or support cells in these structures. These clustered into twelve clusters which could be matched to both functional type and anatomical location. Our data show that dry, moist and hygrocool neurons in chambers I and II are transcriptomically distinct suggesting a functional distinction between these otherwise similar cell types. Furthermore, we identify several candidate genes that may have a role in the function of these cells, including the unknown mechanism of hygrosensory transduction.

Results

Identification of arista and sacculus cells. To build a transcriptomic atlas of the cells in the sacculus and arista we utilized the publicly available Fly Cell Atlas[17]. We started with the available raw data and performed a principal component analysis (PCA) followed by a Nearest Neighbor Clustering using the Seurat pipeline[18,19]. Clustering of all cells resulted in 36 Clusters (Supplemental Fig. 1). Based on differential gene expression in these clusters, we can divide them into 5 functional groups (Fig. 1B): glia cells, marked by the expression of repo[20], muscle cells, marked by expression of Mhc[21], olfactory/temperature/humidity receptor neurons marked by expression of co-receptors Orco, Ir25a and Ir8a[22,23]; Johnston's organ (JO) cells marked by expression of nan, iav, Dnai2 and Dnah3[24], epithelium and support cells marked by expression of shg, sv, snu and osy[25–27]. Similar to the Fly Cell Atlas annotation we are also left with one unidentified cluster. Differential gene expression of highly expressed genes of the unknown cluster shows close similarity to the expression pattern in the clusters assigned as JO cells.

To locate the cells of the sacculus and arista in the dataset we made use of the known expression of Ir93a, Ir40a and Ir21a in these cells[6–9]. We find combined expression of these receptors in only one cluster of the whole antennal dataset, cluster 15 (Fig. 2A). The same cluster also shows expression of arista hot cell marker Gr28b and Ir64a, an acid sensor found in ORNs in sacculus chamber III (Fig. 2A)[10,28]. In chamber III of the sacculus, another olfactory neuron sensing ammonium is also found, defined by co-expression of Rh50 and Amt[11]. These sacculus cells were found in cluster 35.

Apart from neurons, the sacculus and arista sensilla also contain support cells. To identify the sacculus support cells we searched for the known markers Obp59a, CG13258, CG14153 and CG34456[29,30]. While several clusters express Obp59a, at least at low levels, only cluster 28 shows combined expression of Obp59a, CG14153 and CG34456 (Fig. 2A). We therefore exptect cluster 15, 28 and 35 to contain our cells of interest (Fig. 2B).

We extracted all cells from clusters 15, 28 and 35 and sub-clustered them using the Seurat pipeline. This resulted in 12 clusters (Fig. 2C,D). To define these clusters, we looked for expression of previously described markers and could identify the following (Fig. 2D): cluster 0, epithelial cells (based on expression of snu[26,31]); cluster 1, acid sensing cells outside the sacculus (based on expression of Ir75a[23]); cluster 2, acid sensing cells in sacculus chamber III (based on expression of Ir64a[10]; cluster 3, sacculus support cells (based on expression of Obp59a[29,30]); cluster 4, ammonium sensing cells in sacculus chamber III (based on expression of Rh50 and Amt[11]); clusters 5, 8 and 10, dry cells in sacculus chamber I, II and hygrocool cells in chamber II (based on expression of Ir40a[6–9]); clusters 6 and 7: unknown; cluster 9: cold cells in arista and hygrocool cells in sacculus chamber I (based on expression of Ir93a and Ir21a[6–9]); cluster 11, hot cells of the arista (based on expression of Gr28b[14]). We use expression of nSyb to show which clusters have neuronal identity (Fig. 2C). Clusters 6 and 7 likely correspond to moist cells in chamber I and II, however, Ir68a, a receptor previously described as expressed in moist cells[6–9], cannot be found in this sub-clustering and only in 18 cells in the whole antennal dataset. We are therefore disregarding it as a marker gene in this dataset (see Supplemental Fig. 2).

Validation of arista and sacculus cells. To validate the assigned identity we extracted the top 5 markers for each cluster (Fig. 3A). These genes included the known markers for these cells: Gr28b for hot cells (cluster 11), Ir21a for hygrocool cells in chamber I and cold cells (cluster 9), Ir40a for the two dry cell clusters (cluster 5 and 10) and hygrocool cells in chamber II (cluster 8), Ir64 for sacculus acid sensing cells (cluster 2), Ir75abc for Ir75 + cells (cluster 1), Rh50 for ammonium sensing cells (cluster 4), Obp59a for sacculus support cells (cluster 3) and snu for epithelial cells (cluster 0) (Fig. 3A).

To determine the genetic similarities and differences between the clusters we calculated a dendrogram showing the relationships based on the expression of top 100 marker genes (Fig. 3B). This analysis showed that the clusters have pairwise relations relating to their know function: hygrocool cells and arista cold cells in clusters 8 and 9 have closest relation to the hot cells in cluster 11, putative moist cells in cluster 6 and 7 have closest relation to each other, dry cells in clusters 5 and 10 have closest relation to each other, olfactory cells in clusters 1, 2 and 4 have closest relation to each other, and the non-neuronal support cells and epithelial cells have closest relation to each other (Fig. 3B).

Next, we looked at the expression of some of the novel markers identified to validate the identity of the clusters (Fig. 4A–F). We used knock-in Gal4-lines generated to maintain endogenous regulatory sequences reporting the expression of the selected genes crossed to reporters to determine the expression of these genes. 5-HT7 and nAChRalpha6 are both found in cluster 5 and 10 and both genes were expressed in one cell per sensillum in chamber I and II. Additionally, GMR21D03-Gal4, a Gal4-line with expression driven from an enhancer of nAChRalpha6, showed an identical expression pattern in the antenna and stained the VP4 glomerulus in the brain which led us to conclude that clusters 5 and 10 contain dry cells in chamber I and II[32]. Since clusters 5 and 10 are composed of dry cells, cluster 8, the other cluster with expression of Ir40a, contain hygrocool cells in chamber II. Pdfr also showed expression in cluster 8, and the hot cell cluster 11. Pdfr-Gal4 crossed to UAS-CD8::GFP stained cells in the arista and chamber II confirming the identity of cluster 8 as belonging to cells in chamber II. Cluster 6 shows specific expression of Octbeta2R and staining for Octbeta2R > V5 specifically labeled cells in chamber II (Fig. 4C). Co-staining with Ir40a > HA showed that Octbeta2R and Ir40a are not expressed in the same cells and cluster 6 therefore represents moist cells in chamber II. CG42458 is found in cluster 7, 9 and 11. The gene is expressed in the arista, corresponding to cluster 11, and in two cells per sensillum in chamber I. Since cluster 9 contain hygrocool cells in chamber I, cluster 7 likely corresponds to moist cells in chamber I. CG42458, and Pdfr, are both also expressed in support cells surrounding the sacculus corresponding to their expression in cluster 3.

Cluster 9 is a mix of cold cells of the arista and hygrocool cells. The top marker for this cluster, Ir21a, is expressed in both cell types. Expression analysis of another marker for this population, Dh-31R, showed expression in only chamber I, confirming that cluster 9 is a mixed population. To test if we could separate the cold cell

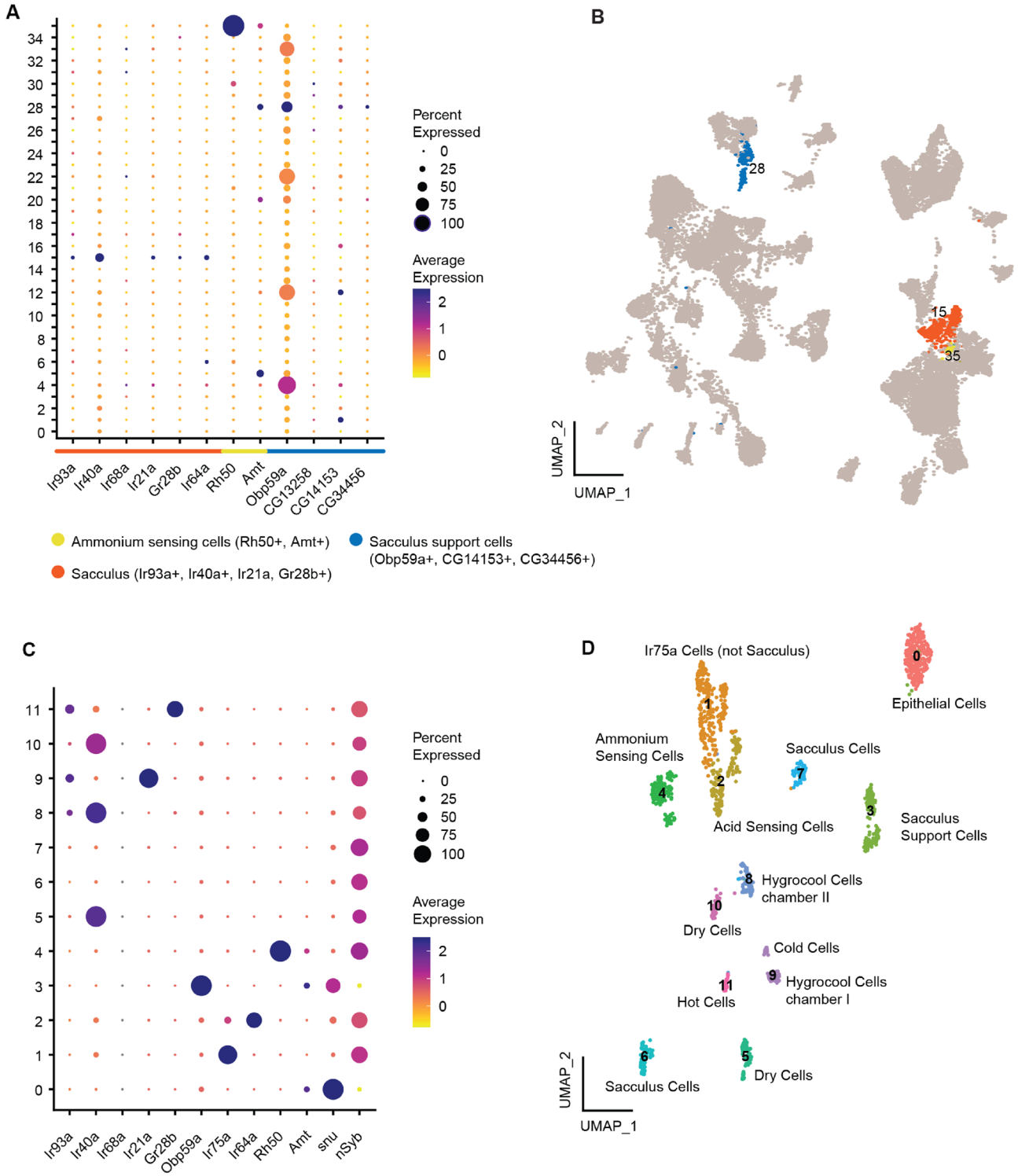

Figure 2. (**A**) Selection of clusters from full antenna dataset for sub-clustering. Dot plot shows expression of known marker genes: expression of Ir93a, Ir40a, Ir21a, Gr28b and Ir64a for sacculus (chamber I, II and III) and arista cells. Co-expression of Rh50 and Amt for ammonium sensing cells (sacculus III). Obp59a, CG13258, CG14153 and CG34456 for sacculus support cells. Based on these expression patterns cluster 15, 28 and 35 were selected for sub-clustering. (**B**) UMAP projection of the full antennal dataset with cluster 15, 28 and 35 highlighted in the colours corresponding to (**A**-**C**) Dot plot of known marker genes in the sub-clustering resulting in 12 clusters. All genes have previously been reported as marker genes for cell identities. We use expression of snustorr (snu) to show epithelial identity and expression of neuronal synaptobrevin (nSyb) to show neuronal identitiy. (**D**) UMAP projection of the 12 clusters with assumed identities based on gene expression from B.

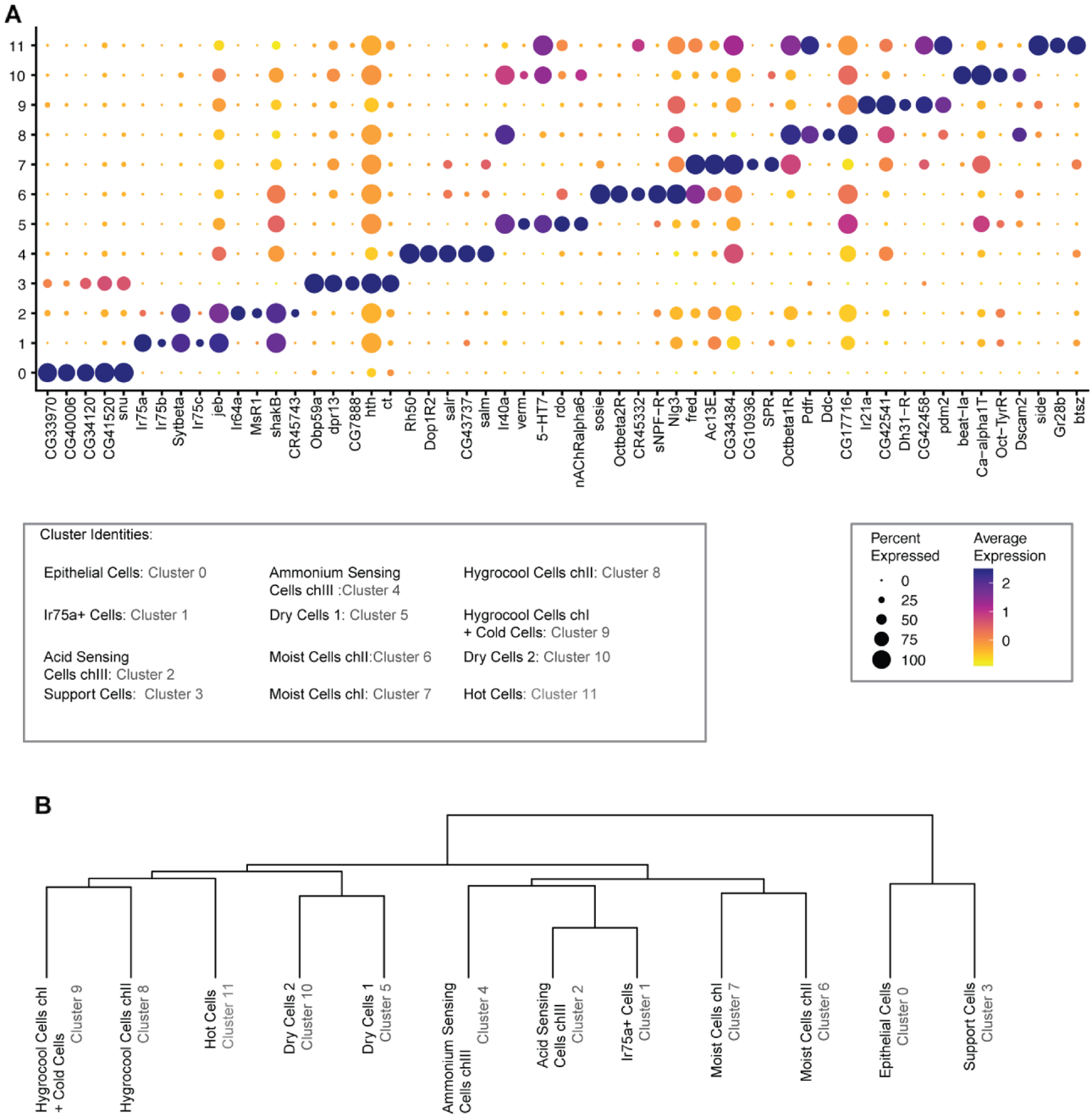

Figure 3. (**A**) Top 5 marker genes for each cluster. The identity and cluster number (in grey) for each group is indicated below. (**B**) Dendrogram indicates the relationship between clusters based on expression patterns of the top 100 genes of each cluster.

and hygrocool cell in chamber I, we extracted the clusters with temperature-sensitive cells, clusters 8, 9 and 11 and performed a sub-clustering. This resulted in four clusters defined by the expression of Ir21a, Gr28b, Ir40a and Dh31-R respectively, suggesting they represent cold cells, hot cells and hygrocool cells in chamber II and I (Supp Fig. 3).

Genetic profile of arista and sacculus cells. Next, we looked at the genes defining each cluster (for top 50 marker genes refer to: Supp Fig. 4—Supp Fig. 8). To determine gene expression patterns that may underlie the functional differences between the cells in the arista and sacculus, we examined the expression patterns of four categories of genes important in shaping a neuronal phenotype: ion channels, GPCR signaling, synaptic vesicle cycle proteins and cell adhesion molecules. We used the top 100 marker genes defining each cluster using the average log2FC value and classified them with gene ontology, GLAD and Flybase terms using the PANGEA tool[33]. After correcting for genes present in more than one cluster, 819 genes were used in the analysis. 48 of these

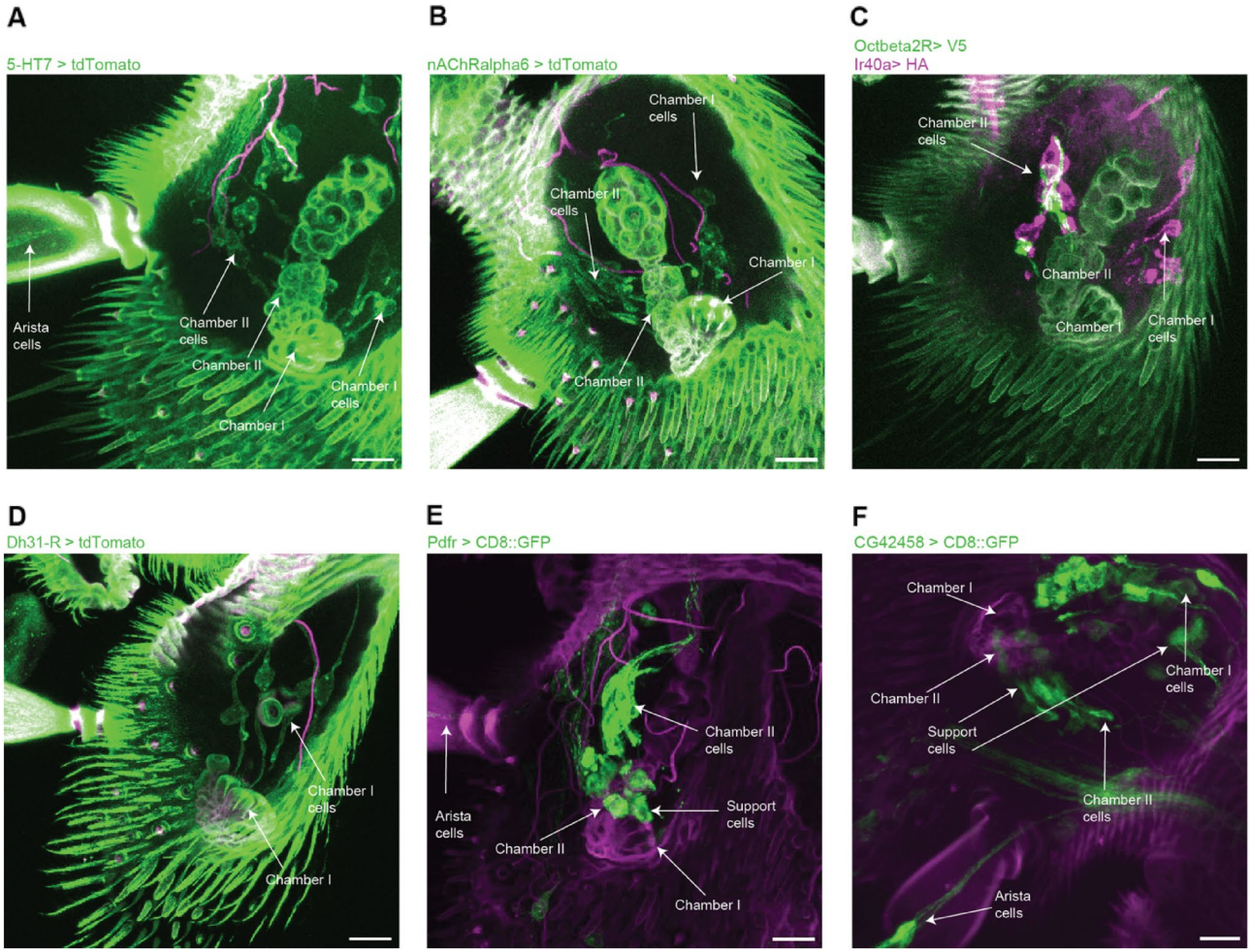

Figure 4. (**A**-**F**) Expression patterns of novel markers in the antenna. Gal4- or LexA-driven expression of reporter genes in green or red and cuticular autofluorescence in magenta. Scale bars indicate 10 mm.

were classified as ion channels, 52 as involved in GPCR signaling, 68 involved in synaptic vesicle cycle and 34 as cell adhesion molecules.

Ligand-gated and voltage gated ion channels comprised the majority of ion channels. Ligand-gated channels showed the greatest specificity within the HRNs and TRNs (Fig. 5). The glutamate receptors Glucalpha and GlurIB are enriched in dry cells and cold cells respectively while the nicotinic receptors nAChRalpha6and nAChRalpha7are enriched in dry cells and moist cells. The voltage-gated channels are more generally expressed between the neuronal clusters except for the Ca^{2+}-channel Ca-alpha1T that is enriched in dry cells and K^{+}-channel Shawl that is enriched in ammonium-sensing cells in chamber III. One TRP channel, Trpm, is enriched and expressed by HRNs in chamber II.

Of the enriched GPCRs, the majority are receptors for neurotransmitters ($n = 15$) or neuropeptides ($n = 14$) (Fig. 6). The neurotransmitters include receptors for dopamine, GABA, acetylcholine, serotonin, tyramine and octopamine. Notably, all octopamine receptors annotated in the *D. melanogaster* genome are expressed in the sacculus in a subtype-specific pattern. Neuropeptide receptors are subtype-specific and most neuronal cell types in the arista and sacculus have a unique expression of one or more neuropeptide receptors. In dry cells an orphan GPCR, CG43795, is specifically enriched. We also find specific expression of several intracellular components of G-protein signaling such as the adenylate cyclases Ac13E and Ac76E.

Genes relating to the synaptic vesicle machinery make up the largest number of genes among those defining the separate clusters (Fig. 7). Fourteen of these genes belong to a family of synaptic adhesion molecules called Defective proboscis extension response (Dpr) and Dpr-interacting proteins (DIPs). Different members of Dprs and DIPs form hetero- and homophilic interactions with each other and are expressed in a subtype-specific pattern. Another family of synaptic adhesion proteins that are part of the synaptic vesicle cycle are neuroligins. They show a subtype-specific pattern with an enrichment of Nlg2 in dry cells and Nlg4 in temperature-sensing cells. We also see an enrichment of the neuronal calcium sensor Frq2 in moist cells and hygrocool cells in chamber II.

Among the cell adhesion molecules, a great diversity of specific expression is observed (Fig. 8). Members of the BEAT and SIDE family of adhesion molecules are expressed in a subtype-specific pattern with Beat-Ia enriched in dry cells and Beat-IIb enriched in hygrocool + cold cells. Side is enriched in hot cells and Side-V in

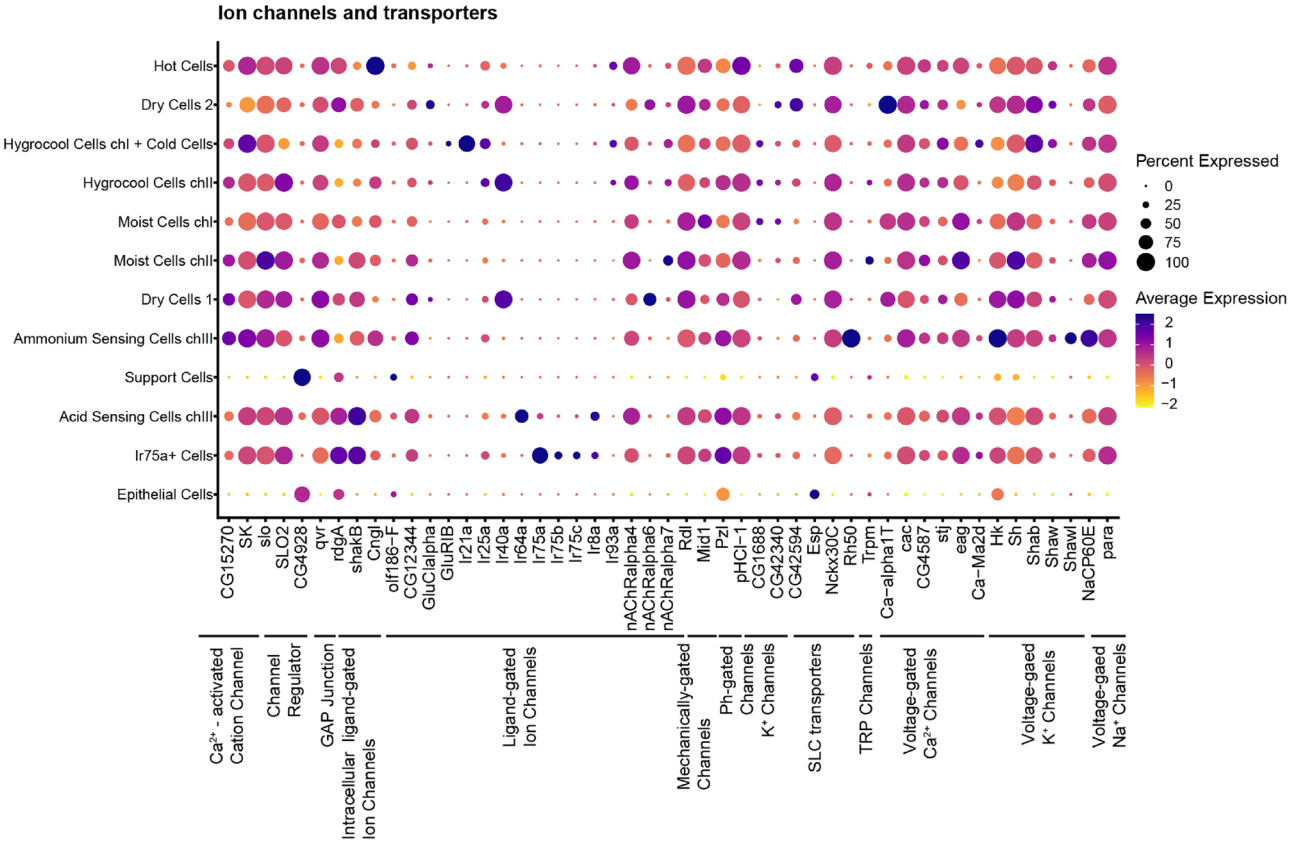

Figure 5. Ion Channels. Dot plot showing expression of selected ion channels. Classification of genes is indicated by the black lines. The size of the dot indicates the fraction of cells in each cluster expressing the genes. The average gene expression for each cluster is shown as a heatmap.

hygrocool cells of chamber I. Dscam2 and Dscam4 as well as the cadherin CadN2 are also expressed in unique patterns.

Enrichment of genes involved in cuticle development. The arista and hygrosensilla both have unique structural features of their overlying cuticle that may be related to its function. We therefore looked at genes involved in cuticle development in our dataset (Fig. 9). Fourteen of the genes enriched are related to the GO term "cuticle development". This includes transcription factors, secreted molecules, enzymes and receptors. Most cuticle development-genes are enriched in the support cells, which are the primary cells responsible for building and maintain the cuticle. However, a few cuticle-related proteins also show specific enrichment in HRNs. The cell adhesion molecule fred is specific for moist cells and the chitin deacetylase verm is specific for dry cells.

Discussion

The current study presents the first comprehensive transcriptomic atlas of the thermosensory and hygrosensory organ of adult *Drosophila melanogaster* with single-cell resolution. By performing unbiased clustering of more than 37,000 nuclei based on their patterns of gene expression, we identified 1411 nuclei that distributed into 12 distinct clusters of cells expressed in the sacculus and the arista. These clusters could be related to a known cell-type based on known markers and novel markers identified in this study. Furthermore, we identified and functionally annotated a large number of genes that were differentially expressed in each cluster compared to all other clusters. This dataset provides a resource for investigating genes involved in thermo- and hygrosensation in insects.

Genetic profile of sacculus and arista cells. Our analysis revealed that the cells of the sacculus and arista can be identified by a unique transcriptomic profile. Thus, despite showing a similar response to a humid stimulus, expressing the same IRs and projecting to the same glomerulus in the antennal lobe, the dry neurons in chamber I and II have unique transcriptomic profiles suggesting they also have unique functions in hygrosensation. Similar observations were made for the other cell types studied. Comparing the uniques transcriptomic profiles we found that the cells responding to a similar stimulus are more similar to each other, thus dry neurons in chamber I and II are more similar to each other than other sacculus or arista cells. Hygrocool cells and the TRNs of the arista group together, likely because they all are thermosensitive neurons.

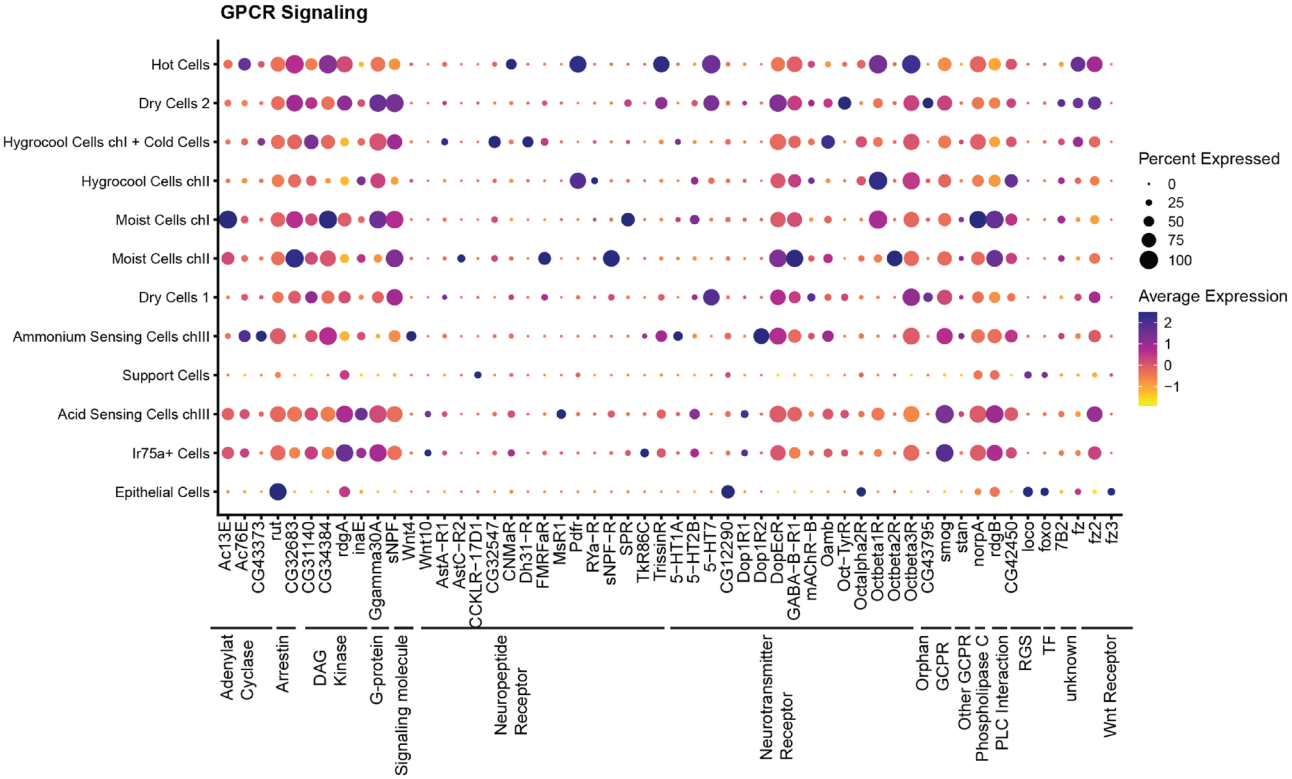

Figure 6. GPCR signalling. Dot plot showing expression of selected genes involved in G protein coupled receptor signalling. Classification of genes is indicated by the black lines. The size of the dot indicates the fraction of cells in each cluster expressing the genes. The average gene expression for each cluster is shown as a heatmap.

Looking at the genes expressed specifically by these cell types we found that dry cells have enriched expression of nAChRalpha6, 5-HT7, Verm, Glucalpha, CG43795 and Oct-TyrR compared to other cells. In moist cells, we only find enriched expression of fred in both chambers. For the hygrocool cell clusters we cannot find any common unique genes between cells of chamber I and chamber II.

Of the genes enriched in arista and sacculus cells we find a large number of genes from the immunoglobulin superfamily. Dprs, DIPs, DSCAM, Beat and Side family members are unique markers for all populations of cells in the sacculus and arista. Members of these gene families interact with each other in a subtype-specific manner during development of the nervous system to establish neuronal connectivity[34–36]. The finding that this expression is maintained in the adult nervous system suggests these genes have a role in the maintenance and structure of the nervous system[37].

Neuropeptides and neurohormones play key roles in the animal's overall regulation of metabolism, physiology, and behavior, acting as global organizers at a higher hierarchical level[38]. We have found expression of several neuropeptide receptors in the sacculus and arista. It includes receptors involved in regulating circadian rhythms, feeding behavior and courtship such as Pdfr, sNPF-R and SPR[39–41]. These behaviors are known to be modulated by temperature and humidity. By identifying the subtype-specific expression of these receptors, the molecular and cellular components of temperature and humidity detection underlying the impact of temperature and humidity on these behaviors can be unraveled.

Other sensory processes like olfaction, gustation and vision are dependent on genes involved in G-protein coupled receptors (GPCRs) . As expected, genes involved in GPCR signaling are also differentially expressed in the hygrosensory and thermosensory neurons of the antenna. Nicotinic acetylcholine receptors (nAChRs) are targets for antiparasitic drugs and insecticides[42,43]. In this dataset we find expression of nAChRalpha4 in all neuronal cells, nAChralpha6 as a distinct marker for the dry cell population and nAChRalpha7 in moist and hygrocool cells.

Neuroligins are post-synaptic adhesion molecules that play a crucial role in synapse forming and maturation[44–46]. In *D.melanogaster* 4 neuroligins have been described: dnlg1-dnlg4 (further referred to as "Nlg1-4")[47,48]. Previous studies describe severely impaired social and mating behavior in flies deficient for Nlg2 and Nlg4[49,50]. Nlg4 is further associated with sleep regulation and flies deficient for Nlg4 show abnormal sleep cycle and circadian rhythm[50,51]. In *Apis mellifera* sensory deprivation in early development changes expression patterns of neuroligins[52]. Here, we find differential expression of Nlg2 (Dry Cells), Nlg3 (Moist Cells chII) and Nlg4 (Hygrocool chI + cold cells and hot cells). To understand the role of neuroligins in humidity sensing and the underlying sensory processes further experiments are required. However, their presence in this group of sensory neurons is further evidence to their involvement in the plasticity of the sensory system.

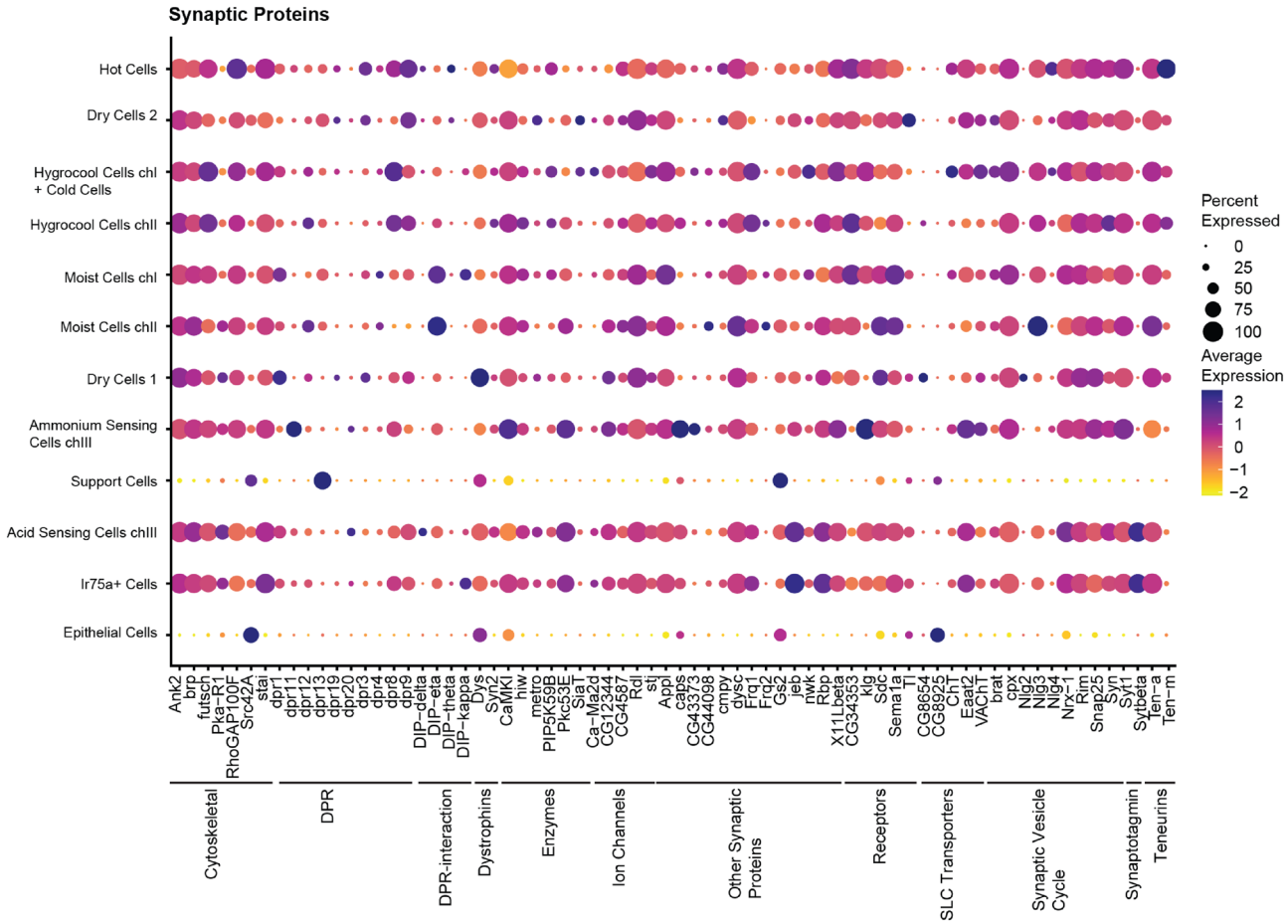

Figure 7. Synaptic Proteins. Dot plot showing expression of selected synaptic proteins. Classification of genes is indicated by the black lines. The size of the dot indicates the fraction of cells in each cluster expressing the genes. The average gene expression for each cluster is shown as a heatmap.

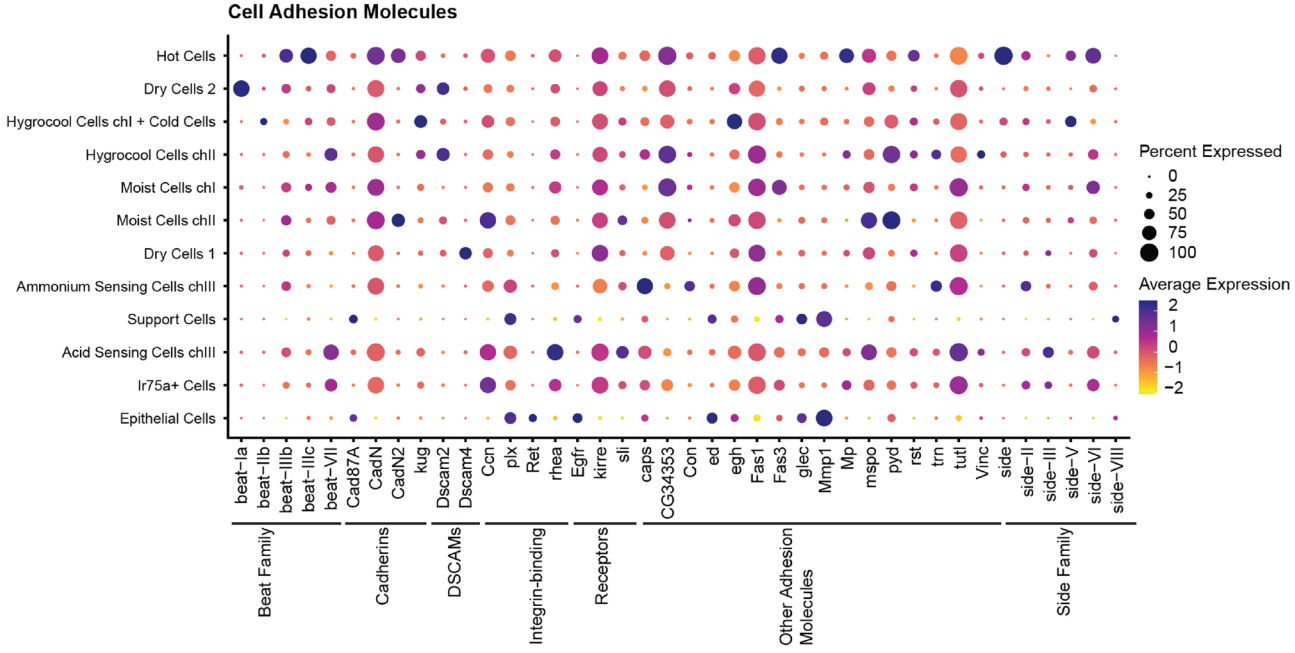

Figure 8. Cell Adhesion Molecules. Dot plot showing expression of selected cell adhesion molecules. Classification of genes is indicated by the black lines. The size of the dot indicates the fraction of cells in each cluster expressing the genes. The average gene expression for each cluster is shown as a heatmap.

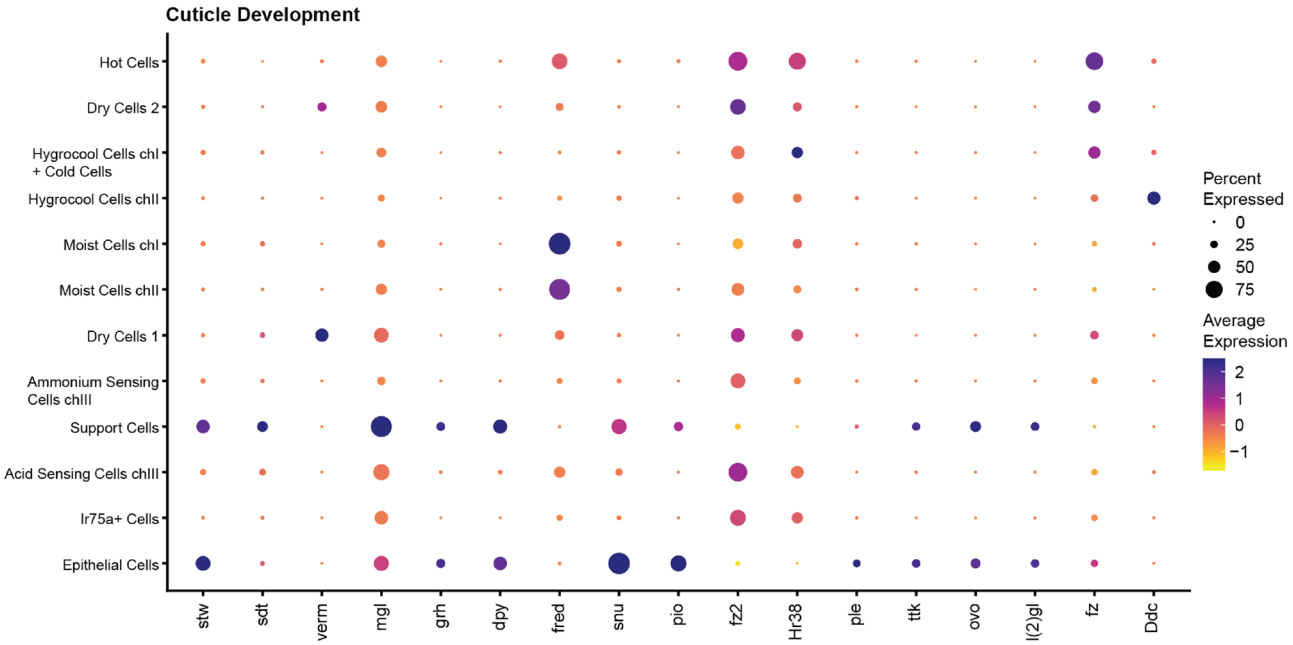

Figure 9. Cuticle Development. Dot plot showing expression of selected genes involved in cuticle development. Classification of genes is indicated by the black lines. The size of the dot indicates the fraction of cells in each cluster expressing the genes. The average gene expression for each cluster is shown as a heatmap.

Concluding remarks

Overall, this dataset provides a valuable resource for future studies aiming for further understanding of the genetic basis of thermosensation and hygrosensation in insects. The identified cell clusters, marker genes, and differentially expressed genes offer new avenues for exploring the intricate mechanisms underlying sensory perception and behavior in response to temperature and humidity cues.

Methods and materials

Animals. All used *Drosophila* strains were raised at 25 °C at a 12:12 h dark/light cycle on standard medium. The following strains were used (Bloomington id number in parenthesis): 5HT7-GAL4 (84,592), nAChRalpha6-GAL4 (84,665), GMR21D03-Gal4 (49,860), Dh31-R-GAL4 (84,625), Pdfr-GAL4 (84,684), CG42458-GAL4 (67,472), Ir68a-GAL4 (91,305), Ir40a-GAL4 (41,727), Octbeta2R-LexA (84,437) and LexAOP-myr::smGdP-V5/UAS-myr::smGdP-HA (76,358).

Single nucleus RNA sequencing analysis. To analyze the transcriptomic profiles of the HRN and TRN population in the *Drosophila* antennae we used the 10 × genomics antennal dataset from the recently published Fly Cell Atlas[17]. Quality control and subsequent analysis was done using the R package Seurat[18,19].

Quality control. The antennal dataset was imported as a Seurat object and then processed using standard quality control metrics. The final data set retains cells expressing more than 200 but less than 2500 genes and less than 5% mitochondria.

This step ensures the quality of the used dataset and excludes possible doublets or damaged cells.

Next, the dataset was normalized by normalizing the gene expression measurement for each individual cell by the total expression, multiplied by a factor of 10,000 and the result log transformed. We then picked the 2000 most variable expressed genes for further analysis. The data was scaled and a principal component analysis (PCA) for the first 40 principal components was calculated.

Nearest neighbor clustering and dimensionality reduction FCA full antennal data set. Unsupervised clustering of the data was done using the standard Seurat clustering approach. Briefly, this uses the Euclidian distance in the pre-defined PCA space (in this case 40 principal components) to compose a K-nearest neighbor (KNN) graph with borders enclosing communities of cells with similar expression patterns. To optimize the standard modularity functions the Louvain algorithm was applied using a resolution of 0.5.

To visualize the resulting clusters the non-linear dimensional reduction UMAP was used with the previously selected 40 PCs.

Assigning cluster identities and identifying the HRNs. To identify the clusters containing the HRN populations we initially searched for known marker genes in the whole antennal neuronal dataset. We then

confirmed these findings by calculating the most differentially expressed genes in those clusters, only reporting the positive markers. Based on this we selected clusters of interest for further analysis.

In the next step we extracted those clusters from the whole data set and ran all commands from normalization to clustering again on this subset of cells.

Here, we again used 40 principal components and a resolution of 0.5, resulting in 12 clusters.

To assign an identity of all resulting clusters we searched for expression of known marker genes for the expected cell types, allowing us to classify all clusters.

Separating the hygrocool cells and temperature cells. In the sub-clustering containing the sacculus and arista cells we can find 3 clusters with assumed thermosensitive identity: arista hot cells, hygrocool cells chII and hygrocool cells ch I + arista cold cells.

To separate the hygrocool cells from the arista cold cells, we extracted those three clusters and followed the Seurat pipeline from normalization to NN clustering. Using 10 principal components and a resolution of 0.7 results in 4 clusters that can be identified as hygrocool cells chI, hygrocool cells chII, hot cells and cold cells.

Selection and classification of differentially expressed features. Each cluster is defined by a set of differentially expressed genes (or biomarkers). Using the Seurat 'FindMarkers' function (with min.pct set to 0.25, reporting only positive markers) returns the markers for each cluster, compared to all remaining cells.

To find the top markers, they were sorted by the average log2FC and the top5, top50 and top100 genes were selected, respectively. The genes listed as top 100 markers were classified with GLAD, Flybase gene group and Gene Ontology term using the PANGEA tool[33].

Visualization of gene expression. To visualize the expression of marker genes across the different clusters, we are using dot plots.

In this style of plot, the average expression of a gene in the cluster is using a heatmap of colors. The size of the dot indicates the percentage of cell express the gene within the cluster. To visualize our data we used the scCustomize package for R[15].

Immunoflourescent stainings. Flies were anesthetized and the antenna dissected. The antennae were fixed in 2% paraformaldehyde (PFA, Electron microscopy studies) in phosphate-buffered saline with 0,5% Triton X-100 (PBST, Sigma-Aldrich) for 55 min at RT and subsequently washed with PBST for 4 × 10 min at RT on a shaker.

Blocking was done using 5% goat serum (Thermofisher) in PBST for 1.5 h at RT and primary antibody was added (GFP A11122 or A11070 Invitrogen, HA-Tag C29F4 Cell signaling technology) diluted 1:300 in 5% goat serum in PBST. The primary antibody is incubated for 4 h on a shaker at RT for 4 h and afterwards for 48 h on 4 °C.

After incubation the samples are washed in PBST 5 × 15 min on a RT shaker secondary antibody (Alexa Fluor 488 goat anti-rabbit IgG A11008 Invitrogen, V5-TAG:DyLight550 MCA1360D550GA Biorad,) diluted 1:500 in 5% goat serum in PBST is added to the samples. The secondary antibody is incubated for 4 h at RT and afterwards for 48-72 h on 4 °C. Samples are washed in PBST 5 × 15 min on a shaker at RT and afterwards mounted with RapiClear (SunJin Lab, Hsinchu, Taiwan, RC149002). Imaging was performed on a Leica SP8 confocal microscope with a 63x, 1.4 NA objective at a resolution of 512 × 512.

Data availability

Data was obtained from https://flycellatlas.org/. In this study we used the 10 × antennal data set in loom-file format. The scripts used for analysis can be found on https://github.com/hygrosensation/D.melanogaster.

Received: 19 June 2023; Accepted: 11 September 2023
Published online: 14 September 2023

References

1. Shelford, V. E. A comparison of the responses of animals in gradients of environmental factors with particular reference to the method of reaction of representatives of the various groups from protozoa to mammaLS. *Science* **48**, 225–230 (1918).
2. Enjin, A. Humidity sensing in insects-from ecology to neural processing. *Curr. Opin. Insect. Sci.* **24**, 1–6 (2017).
3. Okal, M. N., Francis, B., Herrera-Varela, M., Fillinger, U. & Lindsay, S. W. Water vapour is a pre-oviposition attractant for the malaria vector Anopheles gambiae sensu stricto. *Malar. J.* **12**, 365 (2013).
4. von Arx, M., Goyret, J., Davidowitz, G. & Raguso, R. A. Floral humidity as a reliable sensory cue for profitability assessment by nectar-foraging hawkmoths. *Proc. Natl. Acad. Sci. USA.* **109**, 9471–9476 (2012).
5. Altner, H. & Loftus, R. Ultrastructure and function of insect thermo- and hygroreceptors. *Annu. Rev. Entomol.* **30**, 273–295 (1985).
6. Frank, D. D. *et al.* Early integration of temperature and humidity stimuli in the drosophila brain. *Curr. Biol.* **27**, 2381-2388.e4 (2017).
7. Enjin, A. *et al.* Humidity sensing in drosophila. *Curr. Biol.* **26**, 1352–1358 (2016).
8. Knecht, Z. A. *et al.* Distinct combinations of variant ionotropic glutamate receptors mediate thermosensation and hygrosensation in Drosophila. *Elife* **5**, e17879 (2016).
9. Knecht, Z. A. *et al.* Ionotropic Receptor-dependent moist and dry cells control hygrosensation in Drosophila. *Elife* **6**, e26654 (2017).
10. Ai, M. *et al.* Acid sensing by the Drosophila olfactory system. *Nature* **468**, 691–695 (2010).
11. Vulpe, A. *et al.* An ammonium transporter is a non-canonical olfactory receptor for ammonia. *Curr. Biol.* **31**, 3382-3390.e7 (2021).
12. Marin, E. C. *et al.* Connectomics analysis reveals first-, second-, and third-order thermosensory and hygrosensory neurons in the adult drosophila brain. *Curr. Biol.* **30**, 3167-3182.e4 (2020).

13. Budelli, G. *et al.* Ionotropic receptors specify the morphogenesis of phasic sensors controlling rapid thermal preference in Drosophila. *Neuron* **101**, 738-747.e3 (2019).
14. Ni, L. *et al.* A gustatory receptor paralogue controls rapid warmth avoidance in Drosophila. *Nature* **500**, 580–584 (2013).
15. Bates A. antenna. 2021
16. Shanbhag, S. R., Singh, K. & Singh, R. N. Fine structure and primary sensory projections of sensilla located in the sacculus of the antenna of Drosophila melanogaster. *Cell. Tissue Res.* **282**, 237–249 (1995).
17. Li, H. *et al.* Fly Cell Atlas: A single-nucleus transcriptomic atlas of the adult fruit fly. *Science* **375**(6584), eabk2432 (2022).
18. Satija, R., Farrell, J. A., Gennert, D., Schier, A. F. & Regev, A. Spatial reconstruction of single-cell gene expression data. *Nat. Biotechnol.* **33**, 495–502 (2015).
19. Hao, Y. *et al.* Integrated analysis of multimodal single-cell data. *Cell* **184**, 3573-3587.e29 (2021).
20. Halter, D. A. *et al.* The homeobox gene repo is required for the differentiation and maintenance of glia function in the embryonic nervous system of Drosophila melanogaster. *Development* **121**, 317–332 (1995).
21. Paterson, B. M. *et al.* The Drosophila homologue of vertebrate myogenic-determination genes encodes a transiently expressed nuclear protein marking primary myogenic cells. *Proc. Natl. Acad. Sci. USA.* **88**, 3782–3786 (1991).
22. Larsson, M. C. *et al.* Or83b encodes a broadly expressed odorant receptor essential for drosophila olfaction. *Neuron* **43**, 703–714 (2004).
23. Benton, R., Vannice, K. S., Gomez-Diaz, C. & Vosshall, L. B. Variant ionotropic glutamate receptors as chemosensory receptors in Drosophila. *Cell* **136**, 149–162 (2009).
24. Albert, J. T. & Göpfert, M. C. Hearing in Drosophila. *Curr. Opin. Neurobiol.* **34**, 79–85 (2015).
25. Tepass, U. *et al.* shotgun encodes Drosophila E-cadherin and is preferentially required during cell rearrangement in the neurectoderm and other morphogenetically active epithelia. *Genes. Dev.* **10**, 672–685 (1996).
26. Zuber, R. *et al.* The ABC transporter Snu and the extracellular protein Snsl cooperate in the formation of the lipid-based inward and outward barrier in the skin of Drosophila. *Eur. J. Cell. Biol.* **97**, 90–101 (2018).
27. Wang, Y. *et al.* Dysfunction of Oskyddad causes Harlequin-type ichthyosis-like defects in Drosophila melanogaster. *PLoS Genet.* **16**, e1008363 (2020).
28. Thorne, N. & Amrein, H. Atypical expression of Drosophila gustatory receptor genes in sensory and central neurons. *J. Comp. Neurol.* **506**, 548–568 (2008).
29. Sun, J. S. *et al.* Humidity response depends on the small soluble protein Obp59a in Drosophila. *Elife* https://doi.org/10.7554/eLife.39249 (2018).
30. Scalzotto, M. *et al.* Pheromone sensing in Drosophila requires support cell-expressed Osiris 8. *BMC Biology* https://doi.org/10.1186/s12915-022-01425-w (2022).
31. Bray, S. J. & Kafatos, F. C. Developmental function of Elf-1: an essential transcription factor during embryogenesis in Drosophila. *Genes. Dev.* **5**, 1672–1683 (1991).
32. Manning, L. *et al.* A resource for manipulating gene expression and analyzing cis-regulatory modules in the Drosophila CNS. *Cell Rep.* **2**, 1002–1013 (2012).
33. Hu, Y. *et al.* PANGEA: A new gene set enrichment tool for Drosophila and common research organisms. *Nucleic. Acids Res.* https://doi.org/10.1093/nar/gkad331 (2023).
34. Carrillo, R. A. *et al.* Control of synaptic connectivity by a network of drosophila igsf cell surface proteins. *Cell* **163**, 1770–1782 (2015).
35. Tan, L. *et al.* Ig superfamily ligand and receptor pairs expressed in synaptic partners in Drosophila. *Cell* **163**, 1756–1769 (2015).
36. Allen, A. M. *et al.* A single-cell transcriptomic atlas of the adult Drosophila ventral nerve cord. *Elife* https://doi.org/10.7554/eLife.54074 (2020).
37. Nässel, D. R. & Zandawala, M. Hormonal axes in Drosophila: regulation of hormone release and multiplicity of actions. *Cell. Tissue Res.* https://doi.org/10.1007/s00441-020-03264-z (2020).
38. Krupp, J. J. *et al.* Pigment-dispersing factor modulates pheromone production in clock cells that influence mating in drosophila. *Neuron* **79**, 54–68 (2013).
39. Mertens, I., Meeusen, T., Huybrechts, R., De Loof, A. & Schoofs, L. Characterization of the short neuropeptide F receptor from Drosophila melanogaster. *Biochem. Biophys. Res. Commun.* **297**, 1140–1148 (2002).
40. Riva, S. *et al.* Mating disrupts morning anticipation in Drosophila melanogaster females. *PLoS Genet.* **18**, e1010258 (2022).
41. Martin, R. J. Modes of action of anthelmintic drugs. *Vet. J.* **154**, 11–34 (1997).
42. Matsuda, K. *et al.* Neonicotinoids: Insecticides acting on insect nicotinic acetylcholine receptors. *Trends Pharmacol. Sci.* **22**, 573–580 (2001).
43. Varoqueaux, F. *et al.* Neuroligins determine synapse maturation and function. *Neuron* **51**, 741–754 (2006).
44. Chubykin, A. A. *et al.* Activity-dependent validation of excitatory versus inhibitory synapses by neuroligin-1 versus neuroligin-2. *Neuron* **54**, 919–931 (2007).
45. Ichtchenko, K., Nguyen, T. & Südhof, T. C. Structures, alternative splicing, and neurexin binding of multiple neuroligins. *J. Biol. Chem.* **271**, 2676–2682 (1996).
46. Banovic, D. *et al.* Drosophila neuroligin 1 promotes growth and postsynaptic differentiation at glutamatergic neuromuscular junctions. *Neuron* **66**, 724–738 (2010).
47. Sun, M. *et al.* Neuroligin 2 is required for synapse development and function at the Drosophila neuromuscular junction. *J. Neurosci.* **31**, 687–699 (2011).
48. Hahn, N. *et al.* Monogenic heritable autism gene neuroligin impacts Drosophila social behaviour. *Behav. Brain Res.* **252**, 450–457 (2013).
49. Corthals, K. *et al.* Neuroligins Nlg2 and Nlg4 Affect Social Behavior in Drosophila melanogaster. *Front. Psychiatry* **8**, 113 (2017).
50. Li, Y. *et al.* Drosophila neuroligin 4 regulates sleep through modulating GABA transmission. *J. Neurosci.* **33**, 15545–15554 (2013).
51. Biswas, S. *et al.* Sensory regulation of neuroligins and neurexin I in the honeybee brain. *PLoS ONE* **5**, e9133 (2010).
52. Marsh S, Salmon M, Hoffman P. samuel-marsh/scCustomize: Version 1.1.1. 2023

Acknowledgements

We wish to thank the NBIS for their support on this project. The authors thank Marcus Stensmyr for comments on discussion of this project. This project was funded by the WennerGren foundation, Formas—a Swedish Research Council for Sustainable Development, the Swedish Research Council, the Crafoord foundation and the Jaenssons foundation. AC and JR are financially supported by the Knut and Alice Wallenberg Foundation as part of the National Bioinformatics Infrastructure Sweden at SciLifeLab.

Author contributions

A.E. designed the study. K.C. performed the transcriptomic analysis with input from A.C. and J.R. V.A. performed the immunostainings. A.E. and K.C. wrote the manuscript with input from all co-authors.

Funding
Open access funding provided by Lund University. The funding was provided by Wenner-Gren Stiftelserna, Svenska Forskningsrådet Formas (2021-02008), Knut och Alice Wallenbergs Stiftelse, Vetenskapsrådet (2021-03772), Crafoordska Stiftelsen, Jeanssons Stiftelser.

Competing interests
The authors declare no competing interests.

Additional information
Supplementary Information The online version contains supplementary material available at https://doi.org/10.1038/s41598-023-42506-2.

Correspondence and requests for materials should be addressed to A.E.

Reprints and permissions information is available at www.nature.com/reprints.

Publisher's note Springer Nature remains neutral with regard to jurisdictional claims in published maps and institutional affiliations.